



Newtonian and Joule Heating Effects in Two-Dimensional Flow of Williamson Fluid

T. Hayat^{1,2}, A. Shafiq^{1,5†}, M. A. Farooq³, H. H. Alsulami² and S. A. Shehzad⁴

¹ Department of Mathematics, Quaid-i-Azam University 45320 Islamabad 44000, Pakistan

²Nonlinear Analysis and Applied Mathematics (NAAM) Research Group, Faculty of Science, King Abdulaziz University, Jeddah 21589, Saudi Arabia

³Centre for Advanced Mathematics and Physics (CAMP), National University of Sciences and Technology (NUST), Islamabad 44000, Pakistan

⁴Comsats Institute of Information Technology, Sahiwal, Pakistan

⁵ Department of Mathematics, Preston University Kohat Islamabad Campus, Pakistan Regards

†Corresponding Author Email: anumshafiq@gmail.com

(Received January 30, 2015; accepted October 14, 2015)

ABSTRACT

In this article, we have studied the combined effects of Newtonian and Joule heating in two-dimensional flow of Williamson fluid over the stretching surface. Mathematical analysis is presented in the presence of viscous dissipation. The governing partial differential equations are reduced into the ordinary differential equations by appropriate transformations. Both series and numerical solutions are constructed. Graphical results for the velocity and temperature fields are displayed and discussed for various sundry parameters. Numerical values of local skin friction coefficient and the local Nusselt number are tabulated and analyzed.

Keywords: Heat transfer; Joule heating; Williamson fluid; Newtonian heating.

NOMENCLATURE

A_1	first Rivlin Erickson tensor	(u, v)	velocity components
B_0	uniform magnetic field	We	Weissenberg number
C	dimensional constant	(x, y)	spatial co-ordinates
C_{fx}	local skin friction coefficient	ν	kinematics viscosity
c_p	specific heat	f	dimensionless stream function
$(C_i, i = 1-5)$	constants	(f_0, θ_0)	initial approximations of velocity and temperature
Ec	Eckert number	(f_m^*, θ_m^*)	particular solutions of velocity and temperature fields
h_s	heat transfer coefficient	μ_∞	dynamic viscosity
I	identity tensor	μ_0	shear rate viscosity
k	thermal conductivity	ρ	specific heat
L_1, L_2	Linear operators	Γ	time rate constant
M	the Hartman number	\bullet	
Nu_x	local Nusselt number	γ_{ij}	components of shear stress
p	pressure	γ	conjugate parameter
Pr	Prandtl number	θ	dimensionless temperature
q	embedded parameter	Π	second invariant strain tensor
q_w	surface heat flux	η	transformed coordinate
Re_x	local Reynolds number	τ	shear stress
$(\mathbf{R}_m^f, \mathbf{R}_m^\theta)$	m^{th} order nonlinear operators	τ_{xy}	wall shear stress
T	temperature	(h_f, h_θ)	non-zero auxiliary parameters
T_∞	ambient fluid temperature	σ	electrical conductivity
U_w	stretching surface velocity		

1. INTRODUCTION

Boundary layer flows over a stretching surface have great importance in industrial and engineering processes. Such types of flows occur in glass fiber and paper production, extrusion processes, electronic chips, crystal growing etc. (Makinde (2011), Hayat *et al.* (2012) and Turkyilmazoglu and Pop (2013)). On the other hand many researchers are involved to investigate the boundary layer flows of non-Newtonian fluids. This is due to the fact that the rate of heat transfer in non-Newtonian fluid is quite different from those of a Newtonian fluid. Thus several studies dealing with the flow and heat transfer in non-Newtonian fluids exist (Hayat *et al.* (2012), Baoku *et al.* (2013), Rashidi *et al.* (2012), Hayat *et al.* 2012), Shateyi *et al.* (2010), Bhattacharyya *et al.* (2011) and Mukhopadhyay (2013)). It is known that the non-Newtonian fluids in view of their diverse characteristics are already described by many constitutive equations. Williamson fluid is one of the subclasses of non-Newtonian fluids which has not been given due attention. The Cauchy stress tensor in such fluid is

$$\boldsymbol{\tau} = -p\mathbf{I} + \left[\boldsymbol{\mu}_\infty + (\boldsymbol{\mu}_0 - \boldsymbol{\mu}_\infty)(1 - \Gamma\dot{\gamma})^{-1} \right] A_1, \quad (1)$$

where p is the pressure, $\boldsymbol{\mu}_0$ is the zero shear rate viscosity, $\boldsymbol{\mu}_\infty$ is the infinite shear rate viscosity, Γ is the time constant and $\dot{\gamma}$ is defined as

$$\dot{\gamma} = \sqrt{\frac{1}{2} \sum_i \sum_j \dot{\gamma}_{ij} \dot{\gamma}_{ji}} = \sqrt{\frac{\Pi}{2}}, \quad (2)$$

where Π is the second invariant strain tensor. We consider the constitutive equation (1) for the case when $\boldsymbol{\mu}_\infty = 0$ and $\Gamma\dot{\gamma} < 1$. The component of extra stress tensor therefore becomes

$$\boldsymbol{\tau} = \boldsymbol{\mu}_0(1 + \Gamma\dot{\gamma})A_1. \quad (3)$$

where the first Rivlin -Erickson tensor is

$$A_1 = (\text{grad}V) + (\text{grad}V)^*$$

in which (*) denotes the matrix transpose. Quite recently, Dapra and Scarpi (2007) analyzed the perturbation solution for pulsatile flow of a non-Newtonian Williamson fluid in a rock fracture. Noreen *et al.* (2012) investigated the peristaltic flow of a Williamson fluid in an inclined asymmetric channel. Interaction of heat transfer in peristaltic pumping of Williamson fluid in a channel has been studied by Vasudev *et al.* (2010). Nadeem and Akram (2010) have discussed peristaltic flow of Williamson model in an asymmetric channel. Nadeem and Akber (2012) studied the effects of mixed convection heat and mass transfer on peristaltic flow of Williamson fluid in a vertical annulus.

Newtonian heating is the heat transfer rate for which a finite heat capacity is proportional to the local surface temperature from the bounding

surface. It is usually known as the conjugate convective flow. Salleh *et al.* (2010) considered the steady mixed convection boundary layer flow about a solid surface generated by Newtonian heating in which the heat transfer from the surface is proportional to the local surface temperature. They solved the problem numerically by using an implicit finite difference scheme known as the Keller-box method. Hayat *et al.* (2012) studied the boundary layer flow and heat transfer in a second grade fluid over a stretching sheet in the presence of Newtonian heating. They noted that temperature profiles and heat transfer rate significantly increase by increasing the conjugate parameter for Newtonian heating. Magnetohydrodynamic three-dimensional flow of couple stress fluid in the presence of Newtonian heating was addressed by Ramzan *et al.* (2013). Niu *et al.* (2010) analyzed the stability of thermal convection of an Oldroyd-B fluid in a porous medium with Newtonian heating.

It is found that the Newtonian heating effects in two-dimensional flow of Williamson fluid over a stretching surface are not reported yet in the literature. Therefore the object of present communication is to study this problem. The series solutions of velocity and temperature are developed by homotopy analysis method HAM (Liao (2012), Hayat *et al.* (2012), Farooq *et al.* (2014), Hayat *et al.* (2014), Rashidi *et al.* (2013), Abbasbandy *et al.* (2013), Turkyilmazoglu (2012), Shafiq *et al.* (2013), Rashidi *et al.* (2014), Motsa *et al.* (2012), Ellahi *et al.* (2012), Hayat *et al.* (2014), Hayat *et al.* (2015), Sheikholeslami *et al.* (2014) and Hayat *et al.* (2015)). The numerical solutions are obtained by MATLAB. The effects of various parameters on the velocity and temperature profiles are discussed through graphs. The skin friction coefficient and local Nusselt number are computed and examined.

2. MATHEMATICAL FORMULATION

We consider the two-dimensional boundary layer flow of an incompressible Williamson fluid. The flow is induced due to the stretching sheet with linear velocity. Constant magnetic field is applied perpendicular to the plane of stretching surface i-e along $y -$ axis. There is no external electric field and thus polarization effects are neglected. Induced magnetic field is ignored subject to the assumption of small magnetic Reynolds number. Heat transfer analysis is carried out in the presence of Newtonian heating. The viscous dissipation and Joule heating effects are present. The governing two-dimensional boundary layer flow equations for the flow under consideration are

$$\frac{\partial u}{\partial x} + \frac{\partial v}{\partial y} = 0, \quad (4)$$

$$u \frac{\partial u}{\partial x} + v \frac{\partial u}{\partial y} = \nu \frac{\partial^2 u}{\partial y^2} + 2M \frac{\partial u}{\partial y} \frac{\partial^2 u}{\partial y^2} - \frac{\sigma B_0^2}{\rho} u, \quad (5)$$

$$u \frac{\partial T}{\partial x} + v \frac{\partial T}{\partial y} = \frac{K}{\rho c_p} \frac{\partial^2 T}{\partial y^2} + \frac{\mu_0}{\rho c_p} \left(\frac{\partial u}{\partial y} \right)^2 + \frac{\nu \Gamma}{c_p} \left(\frac{\partial u}{\partial y} \right)^3 + \frac{\sigma B_0^2}{\rho c_p} u^2, \quad (6)$$

with the boundary conditions

$$u(x, 0) = U(x) = cx, \quad v(x, 0) = 0, \quad \frac{\partial T(x, 0)}{\partial y} = -h_s T, \\ u \rightarrow 0, \quad T \rightarrow T_\infty \quad \text{when } y \rightarrow \infty, \quad (7)$$

where u and v are the velocity components along the x - and y - directions respectively, ρ the fluid density, σ the electrical conductivity of the fluid, ν the kinematic viscosity, C the stretching rate, K the thermal conductivity, T the temperature of the fluid, c_p the specific heat, h_s the heat transfer parameter and T_∞ the ambient temperature.

Using

$$u(x, y) = cx f'(\eta), \quad v(x, y) = -2\sqrt{cx} f(\eta), \quad (8) \\ \theta = \frac{T - T_\infty}{T_\infty}, \quad \eta = \sqrt{\frac{c}{\nu}} y,$$

the incompressibility condition is automatically satisfied while the other equations and boundary conditions give

$$f''' - (f'')^2 + 2ff'' + 2Wef'' - M^2 f' = 0, \\ f'(0) = 1, \quad f(0) = 0, \quad f'(\infty) = 0, \quad (9) \\ \theta'' + 2Pr f' \theta' + Pr Ec f''^2 + We Pr Ec f''^3 + M^2 Pr Ec f'^2 = 0, \\ \theta'(0) = -\gamma(1 + \theta(0)), \quad \theta(\infty) = 0, \quad (10)$$

where prime denotes differentiation with respect to η , Pr the Prandtl number, We the local Weissenberg number, M is the Hartman number, Ec is the Eckert number and γ is the conjugate parameter for Newtonian heating. These quantities are defined as

$$M^2 = \frac{\sigma B_0^2}{\rho c}, \quad \nu = \frac{\mu_0}{\rho}, \quad We = \Gamma U \sqrt{\frac{c}{\nu}}, \quad (11) \\ Pr = \frac{\mu_0 c_p}{K}, \quad Ec = \frac{(cx)^2}{c_p T_\infty}, \quad \gamma = h_s \sqrt{\frac{\nu}{a}}.$$

The skin friction coefficient C_{fx} and the local Nusselt number Nu_x are given by the following expressions

$$C_f = \frac{\tau_{xy}}{\rho (cx)^2}, \quad Nu_x = \frac{x q_w}{K (T - T_\infty)}, \quad (12)$$

in which the wall skin friction τ_{xy} and the wall

heat flux q_w are

$$\tau_{xy} = \left[\mu_0 \frac{\partial u}{\partial y} + \Gamma \mu_0 \left(\frac{\partial u}{\partial y} \right)^2 \right]_{y=0}, \quad (13) \\ q_w = -K \left(\frac{\partial T}{\partial y} \right)_{y=0}.$$

Equations (12) and (13) through dimensionless variables yield

$$(Re_x)^{1/2} C_f = \{1 + We f''(0)\} f''(0), \quad (14) \\ (Re_x)^{-1/2} Nu_x = \gamma \left(1 + \frac{1}{\theta(0)} \right),$$

where $Re_x^{1/2} = \sqrt{\frac{cx^2}{\nu}}$ is the local Reynolds number.

3. METHODS OF SOLUTION

3.1 Homotopy Analytic Solution

The velocity and temperature for homotopy solutions can be expressed in the set of base functions

$$\{ \eta^k \exp(-n\eta) | k \geq 0, n \geq 0 \}, \quad (15)$$

with

$$f_m(\eta) = \sum_{n=0}^{\infty} \sum_{k=0}^{\infty} a_{m,n}^k \eta^k \exp(-n\eta), \quad (16)$$

$$\theta_m(\eta) = \sum_{n=0}^{\infty} \sum_{k=0}^{\infty} b_{m,n}^k \eta^k \exp(-n\eta), \quad (17)$$

where $a_{m,n}^k$ and $b_{m,n}^k$ are the constants. We have chosen the following initial guess $f_0(\eta)$ and $\theta_0(\eta)$ and the auxiliary linear operators L_1 and L_2 from the rule of solution expression and the boundary conditions

$$f_0(\eta) = 1 - \exp(-\eta), \quad \theta_0(\eta) = \frac{\gamma \exp(-\eta)}{1 - \gamma}, \quad (18)$$

$$L_1[f(\eta)] = \frac{d^3 f}{d\eta^3} - \frac{df}{d\eta}, \quad L_2[\theta(\eta)] = \frac{d^2 \theta}{d\eta^2} - \theta. \quad (19)$$

The operators have the following properties

$$L_1[C_1 + C_2 \exp(\eta) + C_3 \exp(-\eta)] = 0, \quad (20)$$

$$L_2[C_4 \exp(\eta) + C_5 \exp(-\eta)] = 0. \quad (21)$$

where C_i ($i = 1 - 5$) are the constants.

3.2 Numerical Solution

Numerical solution is accomplished with MATLAB built-in-function `bvp4c`. `bvp4c` is constructed to solve a boundary value problems (BVPs). The

MATLAB built-in-function *bvp4c* is a higher order finite difference method which implements 3-stage Lobatto IIIa formula. The results obtained with *bvp4c* are highly accurate. The only challenging part while using *bvp4c* is to suggest a suitable initial guess for the ODEs.

4. CONVERGENCE ANALYSIS

The convergence of series solutions and the approximation rate depend upon auxiliary parameters h_f and h_θ . The appropriate values of auxiliary parameters h_f and h_θ are useful to adjust and control the convergence of the obtained solutions. Therefore Fig. 1 includes the h -curves for velocity and temperature fields at 14th order of approximation. It is noticed that the suitable ranges of h_f and h_θ are $-1.7 \leq h_f < -0.5$ and $-1.6 \leq h_\theta < -0.3$.

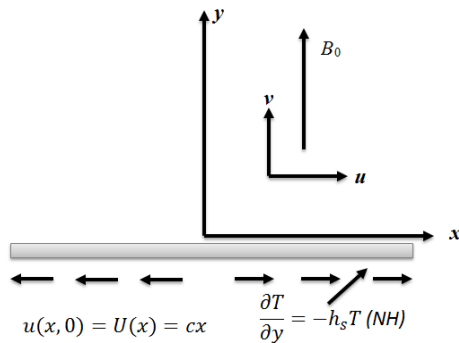


Fig. 1. Flow sketch.

Table 1 Convergence of homotopy solutions when $We = 0.2$, $M = 0.2$, $\gamma = 0.2$, $Pr = 1$, and $Ec = 0.7$.

Order of approximation	$-f''(0)$	$-\theta'(0)$
1	1.1830	0.28635
5	1.4149	0.35999
15	1.4784	0.37516
20	1.4829	0.37550
29	1.4853	0.37559
30	1.4854	0.37559
50	1.4854	0.37559

5. RESULTS AND DISCUSSION

The aim of this section is to examine the effects of Weissenberg number We , Hartman number M , Prandtl number Pr , Eckert number Ec and conjugate parameter of Newtonian heating γ on the velocity and temperature fields. Figs. 2-8 analyze the variations of such parameters. The variation of skin friction coefficient $Re_x^{1/2} C_{fx}$ and the local Nusselt number $Re_x^{-1/2} Nu_x$ for different parameters are also computed in the Tables 2 and 3. Fig. 2 illustrates the influence of Weissenberg

number We on the velocity f' . Clearly f' and the associated momentum boundary layer thickness decrease when We increases. The influence of M on the velocity profile f' is observed from Fig. 3. It has been noticed that the magnetic field retards the flow.

Table 2 Numerical values of skin friction coefficients $Re_x^{1/2} C_{fx}$ for different values of physical parameters.

M	We	$-Re_x^{1/2} C_x$	
		HAM	Numerical
0.1	0.2	1.044	1.044
0.2		1.052	1.052
0.3		1.067	1.068
0.4		1.088	1.088
0.1	0.0	1.178	1.178
	0.1	1.119	1.119
	0.2	1.043	1.043
	0.3	1.001	1.004

Table 3 Numerical values of Nusselt number $Re_x^{-1/2} Nu_x$ for different values of physical parameters.

M	We	Pr	Ec	$Re_x^{-1/2} Nu_x$	
				HAM	Numerical
0.0	0.2	1	0.7	0.4296	0.4295
0.1				0.4279	0.4279
0.2				0.4228	0.4229
0.3				0.4149	0.4150
0.1	0.0	1	0.7	0.4298	0.4298
	0.1			0.4292	0.4293
	0.2			0.4279	0.4279
	0.3			0.4242	0.4242
0.1	0.2	1.0	0.7	0.4279	0.4279
		1.1	0.4354	0.4354	
		1.2	0.4406	0.4405	
		1.3	0.4454	0.4453	
0.1	0.2	1	0.5	0.4779	0.4780
			0.6	0.4505	0.4506
			0.7	0.4279	0.4279
			0.8	0.4090	0.4091

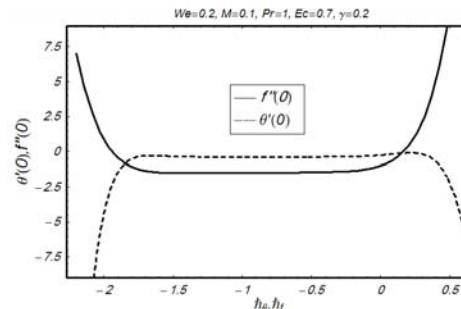


Fig. 2. h -curves for the functions f and θ at 14th-order of approximation.

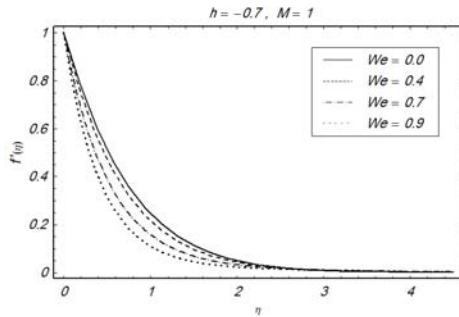


Fig. 3. The influence of We on f' .

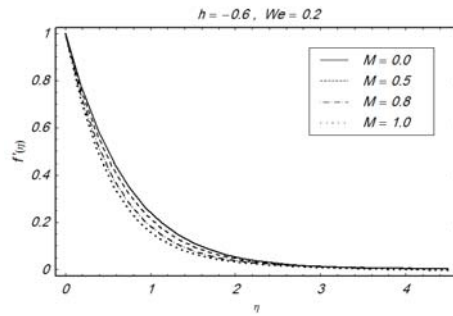


Fig. 4. Influence of M on f' .

Figs. 4-8 show the effects of M , We , Pr , Ec and γ on the dimensionless temperature $\theta(\eta)$. The influence of M on the temperature is observed in Fig. 4. The temperature and thermal boundary layer thickness are increasing function of M . Lorentz force is a resistive force which opposes the fluid motion. As a result heat is produced and thus the thermal boundary layer thickness increases. Magnetic field can control the flow and heat transfer characteristics. Fig. 5 clearly indicates that an increase in the Weissenberg number We leads to a decrease in the temperature profile and thermal boundary layer thickness. Fig. 6 portrays the effects of Pr on $\theta(\eta)$ versus η . It is observed that when we increase the value of Prandtl number Pr the dimensionless temperature $\theta(\eta)$ increases and its related boundary layer thickness is reduced. Physically the Prandtl number is the ratio of momentum to thermal diffusivity. Larger values of Pr has higher momentum diffusivity while smaller thermal diffusivity. This higher momentum diffusivity and smaller thermal diffusivity corresponds to thinning of thermal boundary layer thickness. Figs. 7 and 8 describe the effects of Ec and γ on $\theta(\eta)$ respectively. Both Ec and γ increase the temperature profile $\theta(\eta)$. The Newtonian heating parameter γ depends on the heat transfer coefficient h_s . Increasing in γ leads to an increase in h_s that corresponds to the higher temperature. The numerical values of skin friction coefficient $Re_x^{-1/2} C_{fx}$ and the local Nusselt number

$Re_x^{-1/2} Nu_x$ for different values of M , We , Pr and Ec are computed in the Tables 2 and 3. From Table 2 it is clearly seen that the numerical and analytical solutions are in a very good agreement. The magnitude of skin friction coefficient increases for larger values of M whereas it decreases for We . Table 3 shows that the local Nusselt number increases for larger values of Pr while it has opposite behavior for M , We and Ec . It is also clear from this table that both numerical and analytical solutions are in a very good agreement.

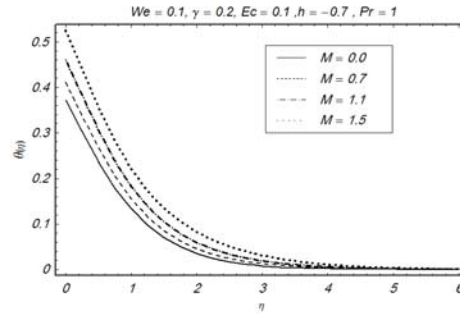


Fig. 5. Influence of M on θ .

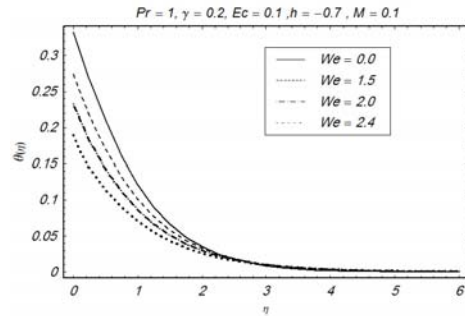


Fig. 6. Influence of We on θ .

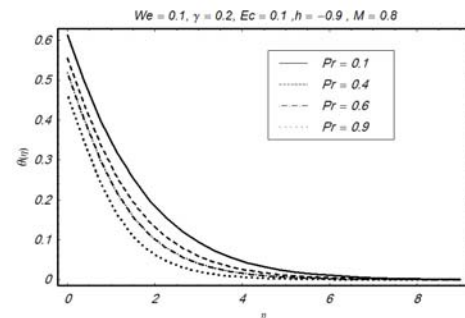


Fig. 7. Influence of Pr on θ .

6. FINAL REMARKS

This attempt examined the influence of Newtonian heating in flow of Williamson fluid over a stretching surface with viscous dissipation and Joule heating. The analytic and numerical solutions have been computed by HAM and the built in

solver `bvp4c` of the software MATLAB respectively. The key points of present study are listed below.

- Table 1 ensures that the convergence of the functions f and $\theta(\eta)$ are obtained at only 24th order of approximation.
- Behaviors of We and M on the velocity and boundary layer thickness are similar.
- Influence of Pr is to decrease the temperature field $\theta(\eta)$ while temperature increases for higher values of Eckert number Ec .
- Skin friction coefficient increases for larger values of M
- Behaviors of M and We on the temperature $\theta(\eta)$ are opposite.
- Analytical results are in an excellent agreement with the numerical solutions for all values of the physical parameters.

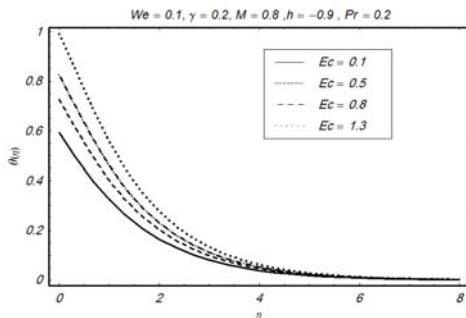


Fig. 8. Influence of Ec on θ .

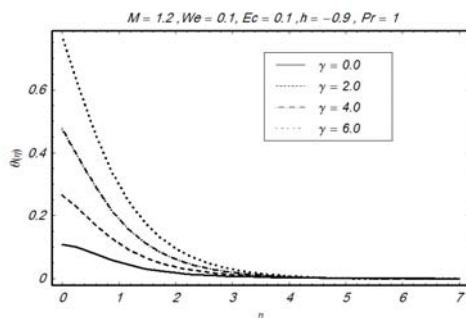


Fig. 8. Influence of γ on θ .

REFERENCES

Abbasbandy, S., M. S. Hashemi and I. Hashim (2013). On convergence of homotopy analysis method and its application to fractional integro-differential equations. *Quaestiones Mathematicae* 36(1), 93-105.

Akbar, N. S., T. Hayat, S. Nadeem and S. Obaidat (2012). Peristaltic flow of a Williamson fluid in an inclined asymmetric channel with partial slip and heat transfer. *Int. J. Heat Mass*

Transfer 55, 1855-1862.

Baoku, I. G., B. I. Olajuwon and A. O. Mustapha (2013). Heat and mass transfer on a MHD third grade fluid with partial slip flow past an infinite vertical insulated porous plate in a porous medium. *International Journal of Heat and Fluid Flow* 40, 81-88.

Bhattacharyya, K., M. S. Uddin, G. C. Layeka and W. Ali Pk (2011). Unsteady helical flows of Oldroyd-B fluids. *Communications in Nonlinear Science and Numerical Simulation* 16, 1378-1386.

Dapra, I. and G. Scarpi (2007). Perturbation solution for pulsatile flow of a non-Newtonian fluid in a rock fracture. *International Journal of Rock Mechanics and Mining Sciences* 44, 271-278.

Ellahi, R., E. Shivanian, S. Abbasbandy, S. U. Rahmanb and T. Hayat (2012). Analysis of steady flows in viscous fluid with heat/mass transfer and slip effects. *International Journal of Heat and Mass Transfer* 55, 6384-6390.

Farooq, U., T. Hayat, A. Alsaedi and S. Liao (2014). Heat and mass transfer of two-layer flows of third-grade nano-fluids in a vertical channel. *Applied Mathematics and Computation* 242(1), 528-540.

Hayat, T, S. A. Shehzad, A. Alsaedi and M. S. Alhothuali (2012). Mixed convection stagnation point flow of Casson fluid with convective boundary conditions. *Chinese Physics Letters* 29, 114704.

Hayat, T., A. Safdar, M. Awais and S. Mesloub (2012). Soret and Dufour effects for three dimensional flow in a viscoelastic fluid over a stretching surface. *International Journal of Heat and Mass Transfer* 55, 2129-2136.

Hayat, T., A. Shafiq and A. Alsaedi (2015). MHD axisymmetric flow of third-grade fluid by a stretching cylinder. *Alexandria Engineering Journal* 54, 205-212.

Hayat, T., A. Shafiq, A. Alsaedi and S. Asghar (2015). Effect of inclined magnetic field in flow of third grade fluid with variable thermal conductivity. *AIP Advances* 5, 087108.

Hayat, T., A. Shafiq, M. Mustafa and A. Alsaedi (2015). Boundary-layer flow of Walters'B fluid with Newtonian heating. *Zeitschrift für Naturforschung A* 70(5), 333-341.

Hayat, T., A. Shafiq, M. Nawaz and A. Alsaedi (2012). MHD axisymmetric flow of third grade fluid between porous disks with heat transfer. *Applied Mathematics and Mechanics (English Edition)* 33, 749-764.

Hayat, T., M. Farooq, Z. Iqbal and A. Alsaedi (2012). Mixed convection Falkner-Skan flow of a Maxwell fluid. *Journal of Heat Transfer* 134, 114504.

Hayat, T., U. Shaheen, A. Shafiq and A. Alsaedi

- and S. Asghar (2015). Marangoni mixed convection flow with Joule heating and nonlinear radiation. *AIP Advances* 5 077140.
- Hayat, T., Z. Hussain, M. Farooq, A. Alsaedi and M. Obaid (2014). Thermally stratified stagnation point flow of an Oldroyd-B fluid. *International Journal of Nonlinear Sciences and Numerical Simulation* 15, 77-86.
- Hayat, T., Z. Iqbal and M. Mustafa (2012). Flow of a Second grade fluid over a stretching surface with Newtonian heating. *Journal of Mechanics* 28, 209-216.
- Liao, S. J. (2012). Homotopy analysis method in nonlinear differential equations. Springer and HigherEducation Press.
- Makinde, O. D. and A. Aziz (2011). Boundary layer flow of a nano fluid past a stretching sheet with convective boundary conditions. *International Journal of Thermal Sciences* 50, 1326-1332.
- Motsa, S. S., S. Shateyi, G. T. Marewo and P. Sibanda (2012). An improved spectral homotopy analysis method for MHD flow in a semi-porous channel. *Numerical Algorithms* 60, 463-481.
- Mukhopadhyay, S. (2013). MHD boundary layer flow and heat transfer over an exponentially stretching sheet embedded in a thermally stratified medium, *Alexandria Engineering Journal* (in press).
- Nadeem, S. and N. S. Akbar (2012). Effects of heat and mass transfer peristaltic flow of Williamson fluid in a vertical annulus. *Meccanica* 47, 141-151.
- Nadeem, S. and S. Akram (2010). Peristaltic flow of a Williamson fluid in an asymmetric channel. *Communications in Nonlinear Science and Numerical Simulation* 15, 1705-1716.
- Niu, J. Fu. C. and W. C. Tan (2010). Stability of thermal convection of an Oldroyd-B fluid in a porous medium with Newtonian heating. *Physics Letters A* 374, 4607-4613.
- Ramzan, M., M. Farooq, A. Alsaedi and T. Hayat (2013). MHD three dimensional flow of couple stress fluid with Newtonian heating. *European Physical Journal Plus* 128, 49.
- Rashidi, M. M., G. Domairry and M. T. Rastegari (2012). Analytical solution for free convection boundary-layer over a vertical cone in a Non-Newtonian fluid saturated porous medium with internal heat generation. *World Applied Sciences Journal* 16, 64-74.
- Rashidi, M. M., M. Ali, N. Freidoonimehr and F. Nazari (2013). Parametric analysis and optimization of entropy generation in unsteady MHD flow over a stretching rotating disk using artificial neural network and particle swarm optimization algorithm. *Energy* 497-510.
- Rashidi, M. M., S. C. Rajvanshi, N. Kavyani, M. Keimanesh, I. Pop and B. S. Saini (2014). Investigation of heat transfer in a porous annulus with pulsating pressure gradient by homotopy analysis method. *Arabian Journal for Science and Engineering (AJSE)* 39(6), 5113-5128.
- Salleh, M. Z., R. Nazar and I. Pop (2010). Mixed convection boundary layer flow about a solid sphere with Newtonian heating. *Arc. Mech.* 62, 283-303.
- Shafiq, A., M. Nawaz, T. Hayat and A. Alsaedi (2013). Magnetohydrodynamic axisymmetric Flow of a third-grade fluid between two porous disks. *Brazilian Journal of Chemical Engineering* 30(3), 599-609.
- Shateyi, S. and S. S. Motsa (2010). Variable viscosity on magnetohydrodynamic fluid flow and heat transfer over an unsteady stretching surface with Hall effect. *Hindawi Publishing Corporation: Boundary Value Problems*.
- Sheikholeslami, M., R. Ellahi, H. R. Ashorynejad, G. Domairry and T. Hayat (2014). Effect of heat transfer in flow of nanofluids over a permeable stretching wall in a porous medium. *Journal of Computational and Theoretical Nanoscience* 11, 486-496.
- Turkylmazoglu, M. (2012). Solution of Thomas-Fermi equation with a convergent approach. *Communications in Nonlinear Science and Numerical Simulation* 17, 4097-4103.
- Turkylmazoglu, M. and I. Pop (2013). Exact analytical solutions for the flow and heat transfer near the stagnation point on a stretching/shrinking sheet in a Jeffrey fluid. *International Journal of Heat and Mass Transfer* 57, 82-88.
- Vasudev, C., U. R. Rao, M. V. S. Reddy and G. P. Rao (2010). Peristaltic pumping of Williamson fluid through a porous medium in a horizontal channel with heat transfer. *American Journal of Scientific and Industrial Research* 13, 656-666.